

WASTE HEAT RECOVERY MODELLING OF A RESIDENTIAL-SCALE STATIONARY FUEL CELL SYSTEM

Diana Albani Siqueira

Centro de Pesquisas de Energia Elétrica – CEPEL
Rio de Janeiro (RJ), Brazil, Caixa Postal 68007, CEP 21944-970
dianas@cepel.br

Helcio Rangel Barreto Orlando

Universidade Federal do Rio de Janeiro/Programa de Engenharia Mecânica/COPPE
Rio de Janeiro (RJ), Brazil
helcio@mecanica.coppe.ufrj.br

Evandro Sérgio Camêlo Cavalcanti

Centro de Pesquisas de Energia Elétrica-CEPEL
21.911-590 Caixa Postal 68007 - Rio de Janeiro (RJ)
camelo@cepel.br

José Geraldo de Melo Furtado

Centro de Pesquisas de Energia Elétrica-CEPEL
21.911-590 Caixa Postal 68007 - Rio de Janeiro (RJ)
furtado@cepel.br

Eduardo Torres Serra

Centro de Pesquisas de Energia Elétrica-CEPEL
21.911-590 Caixa Postal 68007 - Rio de Janeiro (RJ)
etserra@cepel.br

Abstract. *The objectives of this work are to describe the implementation of a systemic mathematical model for a residential-scale stationary polymer electrolyte membrane or proton exchange membrane fuel cell (PEMFC) system and to identify its operational parameters required to match the electrical demand and thermal load for a maximum of four persons occupying a dwelling unit. The modeling approach used in this work takes into account the cogeneration of heat and electrical energy by the fuel cell and its reformer. To this end a polymer electrolyte membrane fuel cell model is being developed and the heat recovery model for the exhaust gas has already been validated. The global steady-state analytical model will be based on global balances of physical and electrochemical phenomena taking place in the fuel cell and its ancillary equipment, as well as on some experimental parameters to be determined from the operation of the specific fuel cell system under study, such as open circuit voltage, ohmic resistance and short circuit current.*

Keywords. *Heat Recovery, Fuel Cell, Modelling, Cogeneration, Exhaust gas.*

1. Introduction

In the last years, distributed generation (DG) technologies such as photovoltaics, wind turbines, micro-turbines, reciprocating engines, and fuel cells have been considered as a generation option by utilities and final customers. Because of the electrical sector restructuring, concerns over reliability of supply, environmental policies, and the potential for improved efficiency are some of the driving factors for locating these small-scale (sized from kW to few MW) generation systems close to the point of electrical consumption (El-Khattam & Salama, 2004).

Fuel cells are electrochemical devices that directly convert chemical energy into electric energy and heat. With no internal movable parts, fuel cells operate in a way similar to dry batteries, except that, in order to produce electricity continuously, they need a continuous supply of fuel, usually hydrogen. They work on the principle of an electrolyte charge exchange between a positive electrode (anode) and a negative electrode (cathode). Practical fuel cells are built from an interconnected assembly of single cells into stacks to provide the desired voltage and power output. A fuel cell stack is a collection of anode–electrolyte–cathode structures, in which electrochemical reactions occur. Detailed description of different fuel cell types and their operation can be found in US-DOE (2004).

Theoretically, fuel cells (FC) have electrical efficiency on the order of 40 to 50 %, based on the lower heat value (LHV) of the fuel (US-DOE, 2004). But, in practice the necessity of a reformer to convert the natural gas or propane to hydrogen and an inverter to convert DC electricity to AC power significantly reduce the electrical efficiency of the overall system. Several field demonstrations of residential fuel cell systems, for example, have reported net electrical efficiencies between 20 % and 30 % (Davis et al., 2005). Considering these practical levels for electrical efficiencies,

utilization of only the electrical energy generated by a fuel cell system may be insufficient to justify the initial investment. Consequently, the economic feasibility of fuel cells in residential and small commercial applications will often depend upon what fraction of the fuel cell's considerable heat generation can also be used in meeting the building's thermal (e.g., domestic hot water, space heating) loads.

The interaction between a house's thermal and electrical performance and a FC-cogeneration unit represents a complex thermodynamic system. Furthermore, the factors which affect the performance are numerous, such as: the occupants' electrical and domestic hot water usage patterns; the house's thermal characteristics; weather; the fuel cell's performance characteristics and operational strategies; and the configuration, design, and operation of the other HVAC components (Braun, 2002). Parise et al. (2005) present an overview of innumerable FC-cogeneration systems.

The complex nature of this problem is well suited to simulation. To this end a polymer electrolyte membrane fuel cell (PEMFC) model is being developed and the heat recovery model has already been validated. This thermodynamic model will be useful for analyzing the technical and economic potential of FC-cogeneration systems and as an R&D tool for assessing and optimizing system design variants. Analytical relations based on experimental FC parameters are used to represent the fuel cell's thermal and electrical performance whereas energy balances, mass balances and thermodynamic relations are used to determine the temperature and flow rate of hot product gases entering the cogeneration unit's exhaust-to-water heat exchanger. This approach is well suited to the current state and rapid pace of fuel cell development as the model will make direct use of benchmark test results.

The objectives of this work are to describe the implementation of a systemic mathematical model for a 5 kW residential-scale stationary PEMFC system installed in CEPEL's laboratory and to identify their experimental parameters that will help to define an operating strategy to match the electrical demand and thermal load for a maximum of four persons occupying a dwelling unit.

2. Modelling

2.1 Background

Many fuel cell systems models have been reported in the open literature and some are available commercially. Haraldsson et al. (2004) have proposed a model selection criteria for choosing a fuel cell model and applied these criteria to select state-of-the-art fuel cell models available in the literature and commercially. Also, Haraldsson et al. (2004) recommended that before selecting a fuel cell model, it is important to take the time to clarify what the key features of the desired model are.

Fuel cell models can be classified as analytical, semi-empirical or mechanistic. Mechanistic models can be further subcategorized based on the solution strategy, single-domain or multi-domain (Faghri and Guo, 2005). The multi-domain approach develops and solves separate equations in each region of the fuel cell. The single-domain approach consists of equations governing the entire domain of interest, with source and sink terms accounting for species consumption and generation within the cell. The merits and demerits of each method are discussed in details by Cheddie and Munroe (2005).

PEMFC modeling has received much attention during the last decade, see for example Biyikoglu (2005). Almost all experimental and numerical studies reviewed by Biyikoglu (2005) were dedicated to PEM modelling of fuel cell components and stacks.

On the other hand, there is a need to study the characteristics of the PEMFC and to model it at the system level (Yavarajan & Dachuan, 2004). Recently, Faghri (2006) has also pointed out that it is necessary to develop models at the system level because fuel cells need a balance of plant (pumps, fans, heaters, compressors, heat exchangers, besides others) in order to optimize the fuel cell system integration.

2.2 The proposed model

In our case, the main interest is to develop a PEMFC model at the system level, incorporating details on the performance of each device and how they affect the overall system performance. This model will be helpful to implement techniques to maximize benefits of PEMFC systems for both electrical generation and thermal energy utilization, and to define the associated operating strategies.

A global model information flow approach similar to Braun's model will be used in this project (see Figure 1), which will take into account the cogeneration of heat and electrical energy by the fuel cell and its reformer. Also, experimental fuel cell data, weather data, utility rate, building characteristics, cost data will be all utilized for the model development.

The FC-cogeneration system consists of a fuel cell stack, fuel processor (reformer and shift converter), power conditioner subsystems, thermal management, water management, and air management, as shown in Figure 2. Analytical relations based on experimental FC parameters are used to represent the fuel cell's thermal and electrical performance whereas energy balances, mass balances and thermodynamic relations are used to determine the temperature and flow rate of hot product gases entering the cogeneration unit's exhaust-to-water heat exchanger.

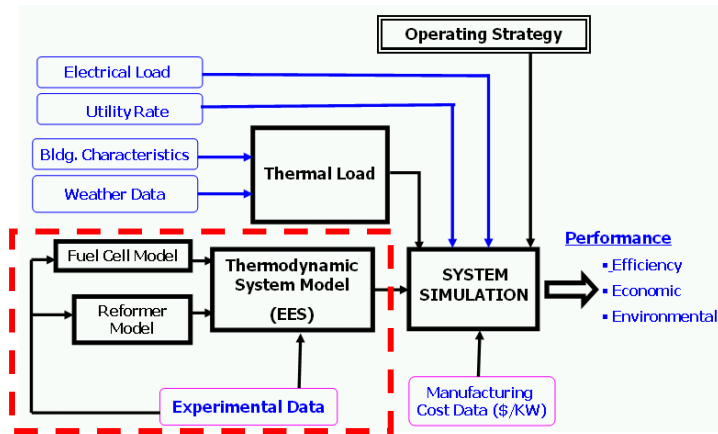


Figure 1. Global model flow approach adapted from Braun (2002).

2.2.1 Electrochemical model

PEMFC fuel cells operate at low temperature (50–90°C), and are fueled using hydrogen or natural gas that has been converted to a mixture of hydrogen and carbon dioxide in the reformer. The reactions occurring in a PEMFC stack proceed as follows



A single cell has an ideal or maximum theoretical thermodynamic efficiency¹ (η_{\max}), for zero power delivery, given by

$$\eta_{\max} = \Delta G / \Delta H_{\text{cell}} \quad (4)$$

where

ΔG is the change in Gibbs free energy of the electrochemical oxidation of the fuel [kJ]

ΔH_{cell} is the change in the reaction enthalpy [kJ].

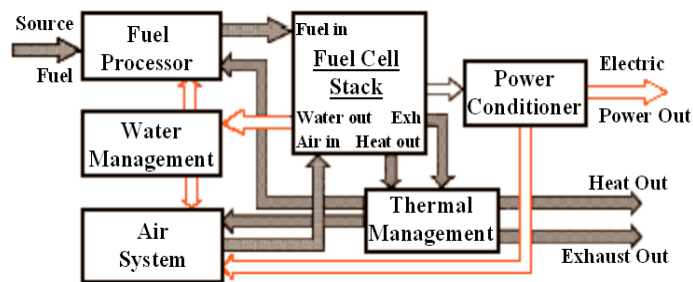


Figure 2. Fuel cell system schematic.

At zero power delivery, the cell losses are also zero and the voltage corresponds to the reversible cell voltage (V_{rev}) or idealised open circuit voltage (OCV)², given by (US-DOE, 2004)

$$V_{\text{rev}} = -\frac{\Delta G}{n \cdot F} \quad (5)$$

where

F is the Faraday constant (96.487 [Coulomb/kmol])

n is the number of electrons given off by one molecule of hydrogen in the fuel cell stack reaction.

¹the ideal or maximum thermal efficiency of a hydrogen/oxygen fuel cell operating reversibly at standard conditions of 25°C (298 K) and 101.3 MPa is 0.83 with liquid water product (US-DOE, 2004).

²OCV for a hydrogen/oxygen fuel cell operating reversibly at standard conditions is 1.23 V with liquid water product, or 1.18 V with gaseous water product (US-DOE, 2004).

When the cell is under load the efficiency and the terminal or actual cell voltage (V_{cell}) decrease in part because of polarization effects. The overall or actual fuel cell efficiency (η_{cell}) is defined as the ratio between the actual cell voltage and the oxidation voltage (V_{ox})³ (Ferguson and Ugursal, 2004)

$$\eta_{cell} = \frac{\text{Useful Work}}{\text{Thermal Energy}} = \frac{V_{cell} \cdot I_{cell}}{\Delta \dot{H}_{cell}} = \eta_{max} \frac{V_{cell}}{V_{rev}} = \frac{V_{cell}}{V_{ox}} \quad (6)$$

where

$\Delta \dot{H}_{cell}$ is the rate of change in reaction enthalpy change [kW]
 I_{cell} is the actual fuel cell current [A].

The ratio between the actual cell voltage and the reversible cell voltage or idealized open circuit voltage is defined as the voltage efficiency (η_v) and can be determined from experimental data obtained during the steady-state operation of the fuel cell under study, as follows

$$V_{cell} = \eta_v V_{rev} \quad (7)$$

So, the actual cell efficiency can be determined by multiplying the voltage efficiency by the maximum theoretical thermal efficiency

$$\eta_{cell} = \eta_v \eta_{max} \quad (8)$$

The inefficiencies associated with polarization effects due to activation, concentration, and ohmic losses, can be determined through the calculation of the voltage efficiency if the fuel cell voltage-current (V - I) characteristic curve is known. In Figure 3 it is presented a typical fuel cell polarization curve (Busquet et al., 2004). In region 1, the voltage decreases drastically due to the oxygen electrochemical activation reactions. In region 2, the curve is roughly linear (resistive loss) and is also known as Tafel region (Ferguson & Ugursal, 2004). Region 3 corresponds to the diffusion loss.

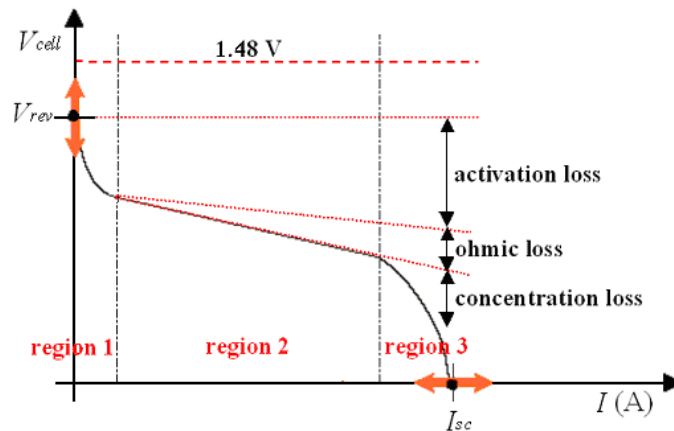


Figure 3. Typical FC V - I characteristic curve adapted from Busquet et al. (2004).

In this project, the works of Ferguson & Ugursal (2004) and Thorstensen (2001) are used as a basis for the steady-state analytical fuel cell model developed. They have demonstrated that the electrochemical model for fuel cell system can be based on the assumption that the fuel cell stack voltage varies linearly with the current. This approach permits the analytical determination of the fuel cell voltage efficiency for a given electrical load.

The approximated polarization curve proposed by Ferguson & Ugursal (2004) and Thorstensen (2001) is determined using only two linear line segments (see Figure 4): the first segment (AB) is a vertical line starting at point A (maximum cell potential at zero current (open circuit condition) and ending at some point B on the vertical axis, and the second segment (BE) is a line collinear with the Tafel portion of the polarization curve that starts at point B⁴ and ending at point E (maximum current (short circuit condition) at zero cell potential). This approach takes in consideration only the activation and ohmic polarizations. The activation loss is accomplished by the introducing a parameter, α , defined as the ratio between the constant activation loss (ΔV_{α}) and the open circuit voltage, as follows

³ 1.48 V, based on the high heating value (HHV) of the fuel (Busquet et al., 2004).

⁴ It is the intersection of the linear approximation to the Tafel region with the voltage axis.

$$\alpha = \frac{\Delta V_{\alpha}}{V_{rev}} = \frac{V_{rev} - V_B}{V_{rev}} \quad (9)$$

being V_B the voltage of point B (see Figure 4) and the ohmic loss by choosing the diagonal line BE with the same slope of the Tafel region, and supposing that the current at point E could be approximated by the short circuit current that occurs at point D.

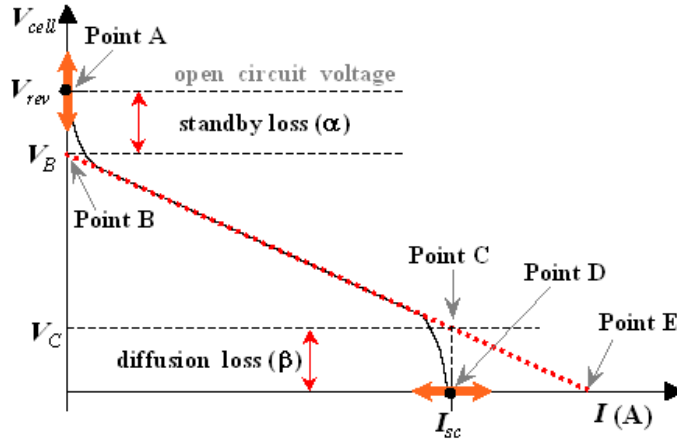


Figure 4. Simplified fuel cell polarization curve.

Considering that the approximation polarization curve proposed by Ferguson & Ugursal (2004) and Thorstensen (2001) doesn't take in consideration the concentration loss characterized by the accentuated voltage drop with current in region 3 (see Figure 3), it is proposed here a modified polarization curve using three linear line segments (AB, BC, CD) that takes in consideration respectively, activation, ohmic and concentration losses. The concentration loss is accomplished by introducing a parameter, β , that describes the ratio between the voltage of point C⁵ and the open circuit voltage, given by

$$\beta = \frac{V_C}{V_{rev}} \quad (10)$$

The modified approximated polarization curve (V - I) depicted in Figure 4 using three linear line segments (AB, BC, CD) as a function of the open circuit voltage, standby loss, diffusion loss and the short circuit current (I_{sc}) is given by

$$I_{cell} = \frac{I_{sc} \cdot (1 - \alpha)}{(1 - \alpha) - \beta} \left(1 - \frac{V_{cell}}{(1 - \alpha) \cdot V_{rev}} \right) \quad (12)$$

Since the gross electrical power (\dot{W}_{gross}) of the fuel cell is the product of current and voltage of each cell multiplied by the number of cells (N) connected in series in the stack, it follows

$$\dot{W}_{gross} = N V_{cell} I_{cell} \quad (13)$$

The rate of enthalpy change required within the cell to produce the gross electrical power can be determined as follows

$$\Delta \dot{H}_{cell} = \dot{W}_{gross} / \eta_{cell} \quad (14)$$

Considering the parasitic electrical consumption (\dot{W}_{para}) associated with ancillary equipment (electrical control system, fans, compressors, pumps, besides others) and the nominal efficiency of the power conditioner (η_{pc}), the actual power delivered by the fuel cell (\dot{W}_{net}), can also be determined

$$\dot{W}_{net} = \eta_{pc} \dot{W}_{gross} - \dot{W}_{para} \quad (15)$$

⁵ intersection of the diagonal BE, colinear with the Tafel portion of the polarization curve, and the vertical through the point D corresponding to the short circuit current at zero cell potential.

As not all of the chemical energy released in the fuel cell stack is converted to electrical work, heat is also produced in the stack. This amount of heat produced in the stack, \dot{Q}_{cell} , can be determined using the calculated actual cell efficiency

$$\dot{Q}_{cell} = \Delta\dot{H}_{cell}(1 - \eta_{cell}) \quad (16)$$

2.2.2 Heat recovery model for the exhaust gas

In addition to the heat recovered from the fuel cell stack, it was also considered here the heat recovery from the exhaust gas. Since hydrogen for the fuel cell is provided by the reform of natural gas, the catalytic reformer is also modeled as part of the whole system. The methods originally proposed by Oshima et al. (1991) for heat recovery from the exhaust gas in a phosphoric acid fuel cell (PAFC) system is extended for PEMFC system in this work, in order to account for non-stoichiometric reactions.

Thanks to the fuel cell voltage-current ($V-I$) characteristic curve it can be determined the corresponding voltage and current for a given gross power generated by the fuel cell. Then, considering that one molecule of hydrogen can give off two electrons in the fuel cell stack reaction, for a given power generated by the fuel cell, the amount of fuel (natural gas) X [kmol/h] to be supplied to the reformer can be expressed as

$$X = \frac{3600 \cdot I_{cell} \cdot N}{2F \cdot 1000 \cdot 4E_h \cdot U} \quad (17)$$

where

E_h is the hydrogen utilization by the fuel cell
 U is the ratio of natural gas being reformed.

Natural gas fuel, mixed with steam, enters the fuel processor where the fuel and steam are catalytically converted into a hydrogen-rich gas. It is assumed that the natural gas is pure methane, also that air is provided to the fuel cell cathode at low pressure (atmospheric) by a blower. The hydrogen-rich gas flows to the fuel cell stack which electrochemically consumes hydrogen from hydrogen-rich gas and oxygen from the air to produce direct current. Water is a byproduct of the electro-chemical process. The depleted fuel leaves the fuel cell stack and flows through the atmospheric vent. Reformer and burner exhaust gas combines with depleted air from the fuel cell stack and flows to the heat exchanger to be cooled for heat and water recovery. The water can be used for fuel processing needs.

Equations (18) to (19) show the chemical reactions that are considered to take place in the fuel processor (reformer and burner) and the fuel cell cathode, taking in account the amount of natural gas X [kmol/h] supplied to the fuel processor and defining: the steam-carbon ratio SPC as the ratio of the amount of steam to the amount of carbon in the fuel that is supplied to the reformer; APF as the air-fuel ratio; E_o as the air utilization, follows for the reformer



for the burner



and for the fuel cell



The compositions and gas flow rates in the PEMFC components are calculated with formulas based on the reactants and products in accord with the chemical reactions presented in equations from (18) to (20).

The heat sources in a PEMFC system are the fuel cell stack and the exhaust gas flow from the reformer and the fuel cell cathode. The heat generated in the fuel cell stack is recovered by a separate coolant. This amount of heat can be calculated with equation (16). Two heat recovery methods from the exhaust gas can be used: one uses heat recovery from mixed exhaust gas from the cathode side of the cells and the reformer, the mixed type as shown in Figure 5; the other uses separate heat recovery from these components, the separate type as shown in Figure 6.

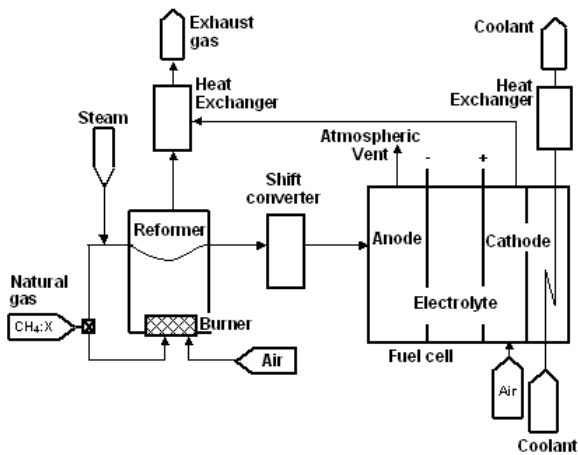


Figure 5. PEMFC system schematic for mixed exhaust gas.

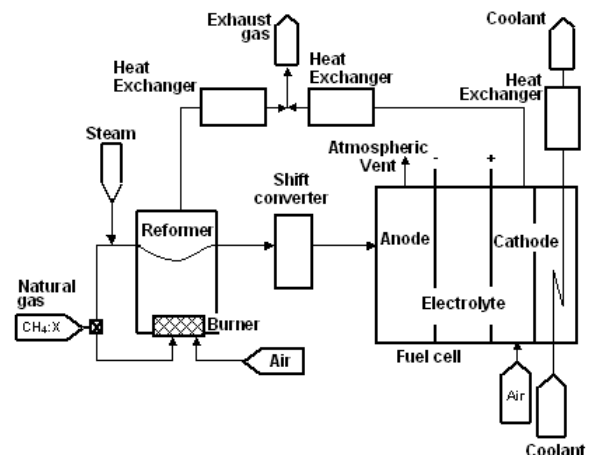


Figure 6. PEMFC system schematic for separated exhaust gas.

The amount of heat recovery from the exhaust gas is calculated from the flow rate and the composition of the gas. This amount of heat is calculated from the sensible and latent heat of the water vapor in the exhaust gas, and also the sensible heat of the exhaust gas excluding the water. The amount of condensate water ($G_w(T)$) [kg/h] at temperature (T) is calculated as follows

$$G_w(T) = G_{H_2O} - \frac{M_w \cdot P_s(T)}{M_a \cdot (P - P_s(T))} \cdot G_a \quad (21)$$

where

- G_a is the mass flow rate of gas without water vapor [kg/h]
- G_{H_2O} is the mass flow rate of water vapor in the exhaust gas [kg/h]
- M_a is the molecular weight of exhaust gas without water vapor [kg/kmol]
- M_w is the molecular weight of water [kg/kmol]
- P is the total pressure of exhaust gas [Pa]
- $P_s(T)$ is the partial pressure of saturate water vapor [Pa]

If the value given by equation (21) is positive, it corresponds to the amount of the condensate water, and if it is negative, it is the sign that the water vapor in the gas does not condense.

In order to calculate the amount of heat recovered from the water vapor, the calculation needs to be separated into two parts: the water vapor in the exhaust gas which condenses, and the water vapor which does not condense.

So, when the dew point temperature of the gas entering the heat exchanger at temperature T_1 is lower than the temperature T_2 at which the gas leaves the heat exchanger, condensation occurs and this temperature corresponds to the value of T for which equation (21) equals to zero. In this case, the amount of heat recovery from the water vapor is calculated adding Q_1 with Q_2 given as follows

$$Q_1 = (h_g(T_1, P_1) - h'(T_2)) \cdot (G_{H_2O} - G_w(T_2)) \quad (22)$$

$$Q_2 = (h_g(T_1, P_1) - h'(T_2)) \cdot G_w(T_2) \quad (23)$$

where

- Q_1 is the sensible heat of non-condensing water vapor [kW]
- Q_2 is the sensible and latent heat of condensed water [kW]
- h' is the specific enthalpy of saturated liquid water [kJ/kg]
- h'' is the specific enthalpy of saturated water vapor [kJ/kg]
- h_g is the specific enthalpy of superheated water vapor [kJ/kg]
- P_1 is the pressure at the heat exchanger inlet [Pa]
- P_2 is the pressure at the heat exchanger exit [Pa]
- T_1 is the exhaust gas temperature at the heat exchanger inlet [°C]
- T_2 is the exhaust gas temperature at the heat exchanger outlet [°C]

On the other hand, when the water vapor does not condense during heat recovery, the amount of heat recovered from the water vapor is calculated from Q_3 given in equation (24)

$$Q_3 = (h_g(T_1, P_1) - h_g(T_2, P_2)) \cdot G_{H_2O} \quad (24)$$

The sensible heat of the exhaust gas excluding the water is calculated as follows

$$Q_4 = c_{p_a}(T_1 - T_2) \cdot G_a \quad (25)$$

where

c_{p_a} is the specific heat at constant pressure of gas without water vapor [kJ/kg.°C]

3. Results and discussions

3.1 Heat recovery model validation

The reformer and fuel cell chemical reactions, energy and mass balances, and also thermodynamic relations used to determine the temperature and flow rate of exhaust gas leaving the exhaust-to-water heat exchanger, were implemented using the EES platform (Klein, 2005), which permits the simultaneous solution of the modeling equations and easily provides physical data for the enthalpy of formation and the enthalpy of the different reactants and products. The simulation is used to calculate the amount of heat recovered from the fuel cell and the reformer exhaust gas for a given electrical power generated by the fuel cell, excluding the heat recovered from the fuel cell stack.

To ensure that heat recovery model results could be legitimately compared to the published results presented in the open literature, the heat recovery model was configured using the simulation conditions used by Oshima et al. (1991) given in Table 1. The calculations were done for two heat recovery methods from the exhaust gas: mixed flow and separated flow. In Figure 7 and 8, the results calculated with the heat recovery methods developed in this paper are compared with the results published by Oshima et al. (1991) respectively, for mixed flow and separated flow. Agreement between the heat recovery model proposed here and Oshima's published results was found to be generally very good, suggesting that the heat recovery model may be used with confidence.

Table 1. Simulations conditions used by Oshima et al. (1991).

DESCRIPTION	VALUE
Steam-carbon ratio (SPC)	3.5
Hydrogen utilization (E_h)	0.8
Air utilization (E_o)	0.5
Air-fuel ratio (APF)	2.0
Fuel cell voltage (V_{cell})	200 [V]
Fuel cell current (I_{cell})	250 [A]
Power (P_{gross})	50 [kW]
Number of cells	300
Temperature of reformer exhaust gas (T_R)	200 [°C]
Temperature of cathode exhaust gas (T_A)	140 [°C]

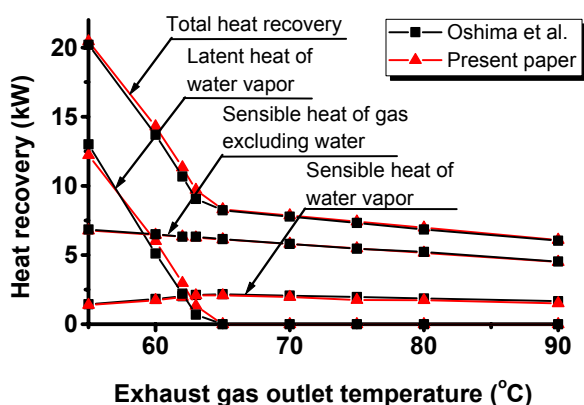


Figure 7. Heat recovery from mixed exhaust gas flow.

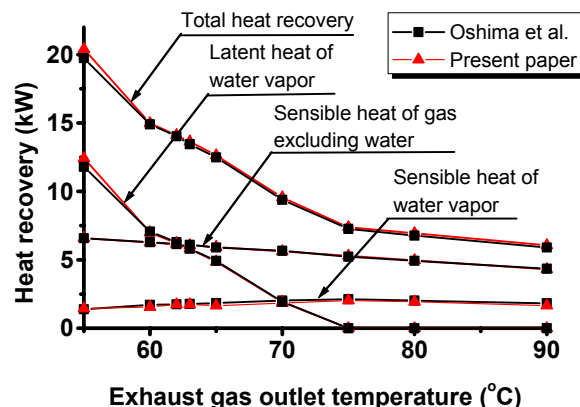


Figure 8. Heat recovery from separated exhaust gas flows.

3.2 Fuel cell case study

The present case study is focused on the operation of a PEMFC produced by a Brazilian fuel cell manufacturer named ELECTROCELL. Figure 9 shows a stand-alone 5 kW electrical power PEMFC system used for benchmark tests at CEPEL's laboratory, adequate to supply power for a maximum of four persons occupying a dwelling unit, has already been commissioned to run directly with hydrogen. The associated steam reformer during the first tests was able to reform 25 liters per minute of natural gas at a pressure of 2 psi to 65-66 liters per minute of hydrogen with only 0.5 ppm of CO, 1.8 ppm of CO₂ e 160 ppm de CH₄ (Serra et al., 2005).

In Figure 10 is shown a preliminary polarization curve for the fuel cell stack, which was extrapolated from the experimental voltage-current characteristics of a single fuel cell.



Figure 9. PEMFC system installed at CEPEL's laboratory: (A) Natural gas reformer; (B) Fuel cell unit and (C) Power conditioner (Serra et al., 2005).

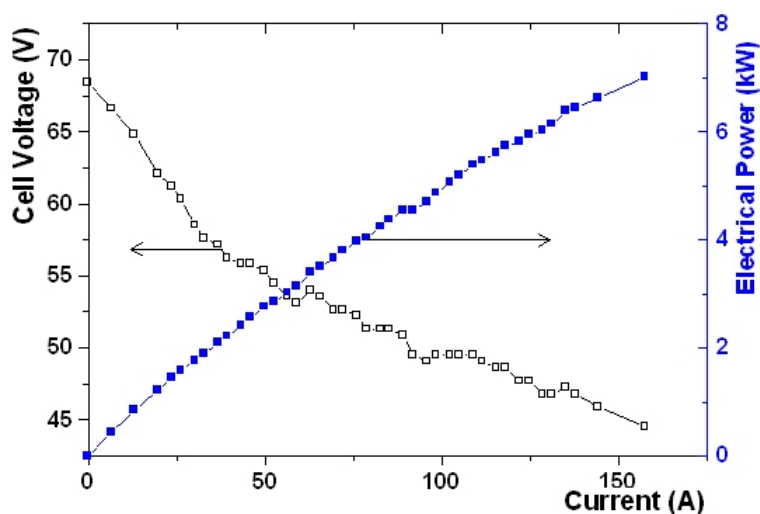


Figure 10. Extrapolated polarization curve for 5kW PEMFC.

The results for the heat recovery from the 5kW PEMFC presented in Figures (11) to (16) are based on the $V-I$ characteristic curve shown in Figure 10, which was used for the determination of each pair of voltage and current for each power level simulated. The simulation conditions used in each calculation are detailed as a legend in each figure.

Two heat recovery strategies were simulated: mixed exhaust gas (see Figure 5) and separated exhaust gas (see Figure 6).

Figure (11) and (12) show the relation between each component of the total heat recovery from the PEMFC exhaust gas, respectively, for mixed type and separated type. As expected, the amount of total heat recovered increases as the exhaust gas outlet temperature decreases for both types. But for the mixed type, see, at around 63°C in Figure (11) the total of heat recovered increase steeply due to water vapor condensation, whereas the sensible heat from the water vapor non-condensing decreases as a consequence of the decreasing of the mass flow rate of water vapor in the exhaust gas flow. Similar effects occur with the heat recovery with the separated type, but because of two independent exhaust gas flow it is verified two inflection points as shown in Figure (12).

Figure 13 presents the comparison of mixed and separated methods of heat recovery for the conditions described in Figures (11) and (12). It shows that the separated method offers between 59.5°C and 75.5°C the possibility to recover more heat than the mixed type, because of the recuperation of latent heat starts early at 75.5°C from the reformer exhaust gas that has a higher dew point than the fuel cell exhaust of the order of 59.5°C.

In Figures (14) to (16) show the heat recovered, according the simulation but varying the following parameters: electrical power load; steam-carbon ratio; air-fuel ratio, respectively. Figure 14 shows that the temperatures at which the two inflection point occur are the same independently of the power generated by the fuel cell.

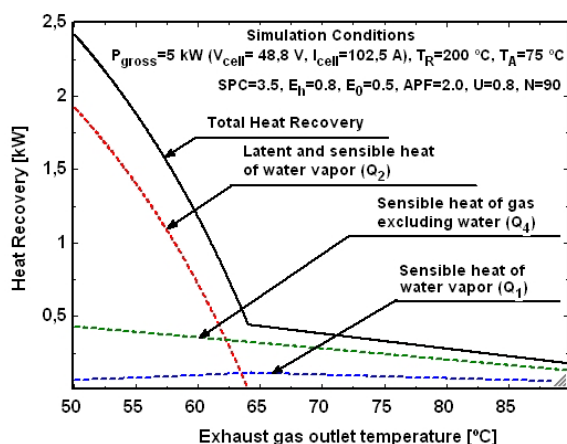


Figure 11. Mixed type heat recovery from PEMFC.

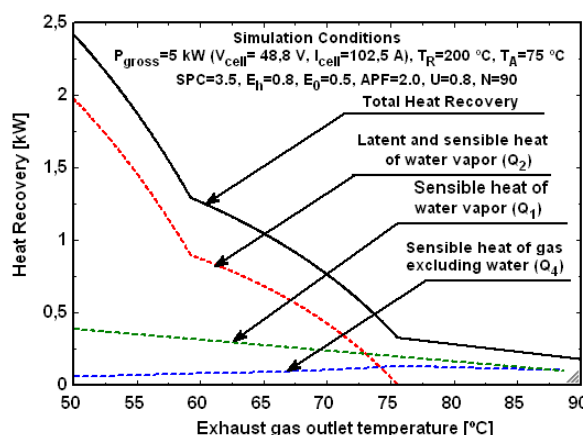


Figure 12. Separated type heat recovery from PEMFC

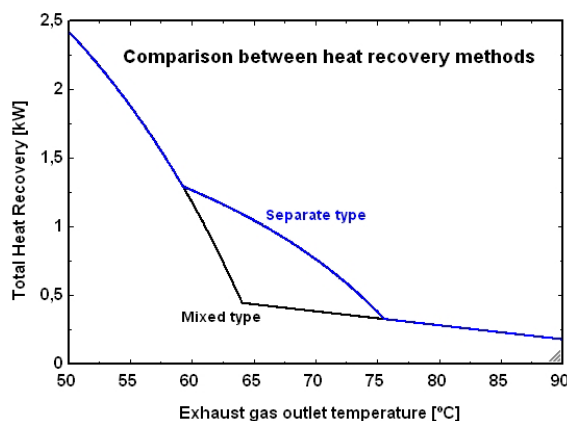


Figure 13. Comparison of heat recovery method types.

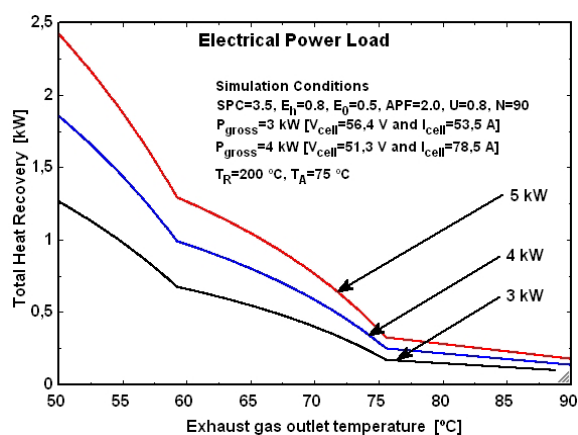


Figure 14. Effect of partial load.

Figure 15 shows that the heat recovered increases as the SPC ratio increases. The amount of steam supplied to the reformer increases with the SPC ratio. Therefore the amount of recoverable latent heat from the water vapor in the reformer exhaust gas increases.

Figure 16 shows that the reformer exhaust gas dew point decreases as the APF ratio increases. As a consequence more heat is recovered from the exhaust gas with lower APF ratio when the exhaust gas temperature leaving the heat exchanger is below the dew point temperature, whereas for temperatures higher than the dew point there is an inversion and more heat is recovered from the exhaust gas as the APF ratio increases. As the air-fuel ratio increases, the mass flow rate of the exhaust gas increases, and also the amount of non-condensing gases (mainly oxygen and nitrogen) increases lowering the partial pressure of the water vapor (lowering the dew point). When the water vapor does not condense, only sensible heat can be recovered. Therefore the amount of heat recovered increases as the mass flow rate of exhaust gas increases.

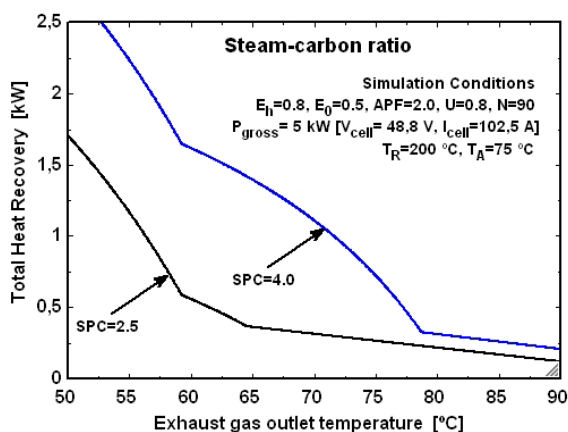


Figure 15. Effect of steam-carbon ratio.

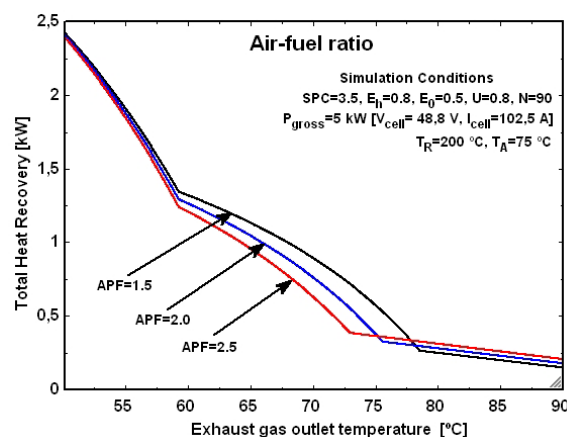


Figure 16. Effect of air-fuel ratio.

4. Concluding Remarks

The results presented here for the heat recovery method, in particular, for the heat recovery separated method from the exhaust gas of a PEMFC system are in total agreement with the results published by Oshima et al. (1991) for heat recovery mixed type from the exhaust gas of a PAFC system. So, it can be expected that the heat recovered from the exhaust gas of other types of fuel cell will present the same behavior.

The heat recovery model for two exhaust gas management strategy from the PEMFC system has been validated. The modules of the fuel cell and of the reformer models are currently being coupled, in order to simulate the behavior of CEPEL's fuel cell for different power levels. Some of the parameters required for the model will be experimentally determined. The model under implementation will be applied to the simulation of such fuel cell, with electrical and thermal demands typical of a Brazilian residential application, keeping in mind that the design of each subsystem must be integrated with the characteristics of the fuel cell stack to provide a complete system. Optimal integration of these subsystems is key to the development of cost effective fuel cell systems.

5. Acknowledgement

The authors greatly acknowledges the support received from The National Fuel Cell Program supported by the Ministério de Ciência e Tecnologia (MCT). Furthermore, the first author acknowledges scholarships received from Centro de Pesquisas de Energia Elétrica (CEPEL) and CNPq (Brazilian Council for Scientific and Technological Development).

6. References

- Biyikoglu, A., 2005, "Review of proton exchange membrane fuel cell models", *International Journal of Hydrogen Energy* **30**: 1181-1212.
- Braun, R.J., 2002, "Optimal Design and Operation of Solid Oxide Fuel Cell Systems for Small-Scale Stationary Applications", PhD Thesis, University of Wisconsin-Madison, USA.
- Busquet, S., Hubert, C.E.; Labbé, J.; Mayer, D.; Metkemeijer, R. 2004. A new approach to empirical electrical modelling of a fuel cell, an electrolyser or a regenerative fuel cell, *Journal of Power Sources*, **134**:41–48, 2004.
- Cheddie, D. and Munroe, N., 2005, "Review and comparison of approaches to proton exchange membrane fuel cell modelling", *Journal of Power Sources*, **147**:72–84, (2005).
- Davis, M.W.; Fanney, A.H.; LaBarre, M.J.; Henderson, K.R.; Dougherty, B.P., 2005, "Parameters Affecting the Performance of a Residential-scale Stationary Fuel Cell System", *Proceedings of FUELCELL2005: Third International Conference on Fuel Cell Science, Engineering and Technology*, May 23-25, 2005, Ypsilanti, Michigan.
- El-Khattam, W. and M.M.A. Salama, 2004, "Distributed generation technologies, definitions and benefits", *Electric Power Systems Research* **71**:119–128.
- Faghri, A. and Guo, Z., 2005, "Challenges and opportunities of thermal management issues related to fuel cell technology and modeling", *International Journal of Heat and Mass Transfer*, **48**:3891-3920.
- Faghri, A., 2006, "Unresolved issues in fuel cell modeling", *Heat Transfer Engineering*, **27**(1):1-3.
- Ferguson, A. and Ugursal, V.I., 2004, "Fuel Cell Modelling for Building Cogeneration Applications", *Journal of Power Sources* **137**:30-42.
- Haraldsson, K.; and Wipke, K., 2004, "Evaluating PEM fuel cell system models", *Journal of Power Sources*, **126**:88–97.

- Klein, S.A., 2005, ESS-Engineering Equation Solver, Manual v7.409-3D, f-Chart Software, Middleton, Wisconsin, 294p..
- Oshima, K.; Uekusa, T.; Ichimura, M.; Koyashiki, T., 1991, “A Study of Heat Recovery from Fuel Cell Exhaust Gas for Telecommunications Equipment Cooling”, 13thInternational Telecommunications Energy Conference, INTELEC'91, 5-8 Nov. 1991, pp 379 – 386.
- Parise, J.A.R.; Vargas, J.V.C.; and Pitanga Marques, R., 2005, “Fuel Cells and Cogeneration”, Proceedings of FuelCell2005: Third International Conference on Fuel Cell Science, Engineering and Technology, Ypsilanti, MI, USA, May 23-25.
- Serra, E.T.; Furtado, J.G.M.; Soares, G.F.W.; Codeceira Neto, A., 2005, “Implementation of a Polymer Electrolyte Membrane Fuel Cell System for Distributed Generation Studies”, Proceedings of SNPTEE2005: Seminário Nacional de Produção e Transmissão de Energia Elétrica, Oct.16-21, Curitiba, Brazil, (in portuguese).
- Thorstensen, B., 2001, “A Parametric Study of Fuel Cell System Efficiency Under Full and Part Load Operation”, Journal of Power Sources 92:9-16.
- US-DOE, 2004, “Fuel Cell Handbook”, 7th Ed., United States Department of Energy, Morgantown,USA.
- Yuvarajan, S. and Yu, D., 2006, “Characteristics and Modeling of PEM Fuel Cells”, ISCAS2004 Proceedings - International Symposium on Circuits and Systems, Vancouver (Canada), pp.V-880:883, May 23-26.

6. Copyright Notice

The authors are the only responsible for the printed material included in their paper.